Worst-Case Analysis of a 3-Frequency Receiver to Land a General Aviation Airplane

Shau-Shiun Jan, Demoz Gebre-Egziabher, Todd Walter, Per Enge
Department of Aeronautics and Astronautics
Stanford University, California 94305

Abstract

This paper investigates the vertical guidance performance of a multiple frequency WAAS receiver (L1, L2, and L5) in the presence of inclement weather and radio frequency interference (RFI). There are several ways to take advantage of the multiple frequencies. For example, one can calculate ionosphere delay in the airplane. This would replace the grid of ionosphere delay corrections used currently by the Wide Area Augmentation System (WAAS). This direct use of multiple frequencies would be more accurate, and offer higher availability. Another way to take advantage of the multiple frequencies is by using the additional GPS frequencies as a backup navigation method when RFI is present. This would require the user to continue using the grid. This paper presents the results of a trade-off study evaluating the performance of various architectures for a multiple-frequency GPS landing system. The architectures evaluated depend on the number of the available GPS frequencies and include the following:

- Case 1: all three GPS frequencies are available,
- Case 2: two of three GPS Frequencies are available,
- Case 3: one of three GPS frequencies is available.

Our criterion is to compare the coverage of availabilities versus the vertical alert limit (VAL) under these three cases.

In addition to the three system architectures, this paper also investigates the effect of using a barometric altimeter. We treat a barometric altimeter as a virtual satellite with a known clock directly above the user's position. Historical meteorological observation data is used to develop a barometric altimeter simulator in MATLAB®. We then compared the estimated altitude with the true altitude to generate altitude error data. We analyze the altitude error data, and calculate the 68% (1σ) and worst-case error bounds in the probability density function (PDF) of the altitude error. We apply a linear least-square estimation technique to the resulting error bounds in different regions, and we build up an altitude error model, which shows that the altitude error is function of the distance between a user and reference location. We evaluated a worst-case model of barometric altimeter based on the historical meteorological observation data.

I. Introduction

In 2005~8, civilians will have access to three GPS signals: L1 (1575.42 MHz), L2 (1227.60 MHz), and L5 (1176.45 MHz) [9]. Both L1 and L5 are for civil aviation safety-of-life services. L2 is for non-safety critical applications. There are several ways to take credit for the new frequencies:

- Calculate ionosphere delay in the airplane - this might eliminate the grid which is used for ionosphere delay corrections in WAAS [2]. As a result, we might have fewer wide area reference stations (WRS). This system might be less expensive.
- When radio frequency interference (RFI) is present, we can use the additional GPS frequencies as a backup navigation method. This system requires WAAS to continue broadcasting the ionosphere grid.
- Combine the above two methods to form a more robust navigation system.

In addition to the multi-frequency GPS and WAAS, this paper also investigates the effect of using a barometric altimeter [5]. As part of this work a barometric altimeter simulator was developed. The simulator was used to estimate altitude from historical meteorological observation data collected at different locations in the Conterminous United States (CONUS) [8]. By comparing the estimated altitude with true altitude, altitude error data was generated. By applying statistical and linear estimation techniques to the altitude error data, a model for barometric altimeter confidence is developed. This barometric altimeter confidence model is evaluated via the historical worst-case meteorological observation data.

This paper is organized as follows. Section II discusses the configuration and assumptions. The basics of barometric altimeters are discussed in Section III. In Section IV, we explain our barometric altimeter error model. Section V describes the parameter changes in calculation of WAAS protection level [7]. A short description of the modified MAAST [4] and analysis of

results of some simulated cases are given in Section VI. Section VII presents a summary and concluding remarks.

II. Configuration and Assumptions

In this work, we assumed that the user is a general aviation (GA) aircraft and is equipped with two available systems: a 3-frequency WAAS receiver, and a barometric altimeter. Because of the presence of bad weather and RFI, a 3-frequency WAAS receiver might lose tracking one or two of three GPS frequencies. Depending on the number of available GPS frequencies, seven potential system configurations are possible, as shown in Figure 1. Only the single frequency cases will be discussed in this paper. The other cases will be the subject of a future paper.

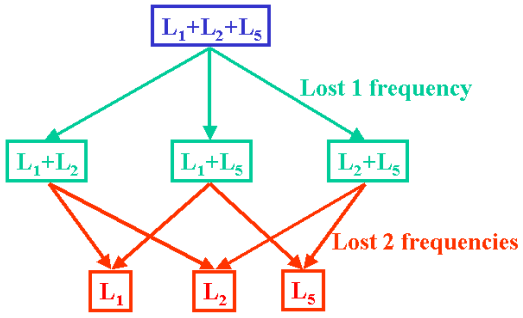

Figure 1. Depending on the number of available GPS frequencies, a 3-frequency WAAS receiver can use these frequencies in one of seven ways.

The three GPS frequencies are the main objective of GPS modernization [9]. In addition to the current GPS which has C/A code on L1, and P(Y) on L1 and L2, there will be a second civil code on L2, and a third civil signal (L5) with new civil code (I, Q) on it. A short description of these three GPS frequencies is as follows:

- The center frequency of L1 is 1575.42 MHz, and the bandwidth is 20MHz. It has C/A and P(Y) codes. The pseudo random noise (PRN) code has a chipping-rate of 1.023MHz [3].
- The center frequency of L2 is 1227.6MHz, and the bandwidth is 20MHz. It has civil code and P(Y) codes. The PRN code on L2 has a same chipping-rate as L1 [3].
- The center frequency of L5 is 1176.45MHz, and the bandwidth is 24MHz. It has I and Q codes. The PRN code on L5 has a chipping rate of 10.23MHz [9].

The Wide Area Augmentation System (WAAS) [2] augments GPS with the following three services:

- Ranging using "GPS-like" signals from geostationary satellites (GEOs) at L1 frequency.
- Accuracy improvements by sending differential corrections via the same GEO signal.
- Integrity by sending integrity message over the same signal.

It should be noted that the current WAAS corrections are specified for L1 only. The other single GPS frequency (L2, or L5) users will require some additional modification before they can apply WAAS corrections to their position-fix. A more detailed discussion is in Section VI.

One assumption that has been made in this paper is that the WAAS corrections are always available to the user, even when the GPS L1 signal is blocked by RFI. This is a reasonable assumption, provided one can leverage the fact that the WAAS messages can also transmitted via GEOs on the other frequencies (L2, L5) or via other network, for example, LORAN (Long Range Navigation).

III. Basics of Barometric Altimeter

In addition to the multi-frequency GPS and WAAS, this paper also investigates the use of a barometric altimeter. Barometric altimeters [10] contain a sealed bellows that expands or contracts in response to the change in air pressure associated with a change in altitude. Gears translate the movement of the bellows into the movement of pointers on a dial, which shows the pilot the altitude of the plane in relation to sea level. A barometric altimeter has a knob that pilots use to adjust for the reference pressure. For airplanes flying at an altitude greater than 18,000 feet above sea level, the normal procedure is to adjust the barometric altimeter to a standard pressure of 29.92 inches of mercury. For airplanes flying at an altitude less than 18,000 feet above sea level, the normal procedure is to adjust the barometric altimeter to the local barometric pressure provided by air traffic control, as illustrated in Figure 2.

The conversion of measured air pressure to altitude is based on a theoretical standard atmosphere and a corresponding pressure versus altitude curve as well as the assumption that air is a perfect gas. More precisely, the standard atmosphere [10] is defined as follows:

- The air is a perfect gas with the gas constant $R=287\ J/Kg/K$.
- The pressure at sea level is $P_0=29.92\ in.\text{-}Hg$.
- The temperature at sea level is $T_0=15^oC$.
- The temperature gradient (lapse rate) is $\lambda=0.0065^oC/m$.

The conversion of measured air pressure to altitude is based on the following equation:

$$h_c = \frac{T_0}{\lambda}\left[1 - \left(\frac{P_m}{P_0}\right)^{\frac{\lambda R}{g}}\right] \quad (1)$$

Where,

h_c : calculate altitude

T_0 : temperature at the level of reference

λ : lapse rate

P_0 : pressure at the level of reference

P_m : pressure measured

R : universal gas constant

g : acceleration of gravity

IV. Barometric Altimeter Error Model

To estimate the accuracy of the barometric altimeter, we developed a barometric altimeter simulator based on the altitude equation (1) by using MATLAB®. The scenario of our simulation is shown in Figure 2. We assumed that an airplane at location B received temperature and pressure data (P_0, T_0) from a reference station (a control tower or a weather station) at location A. This airplane then used these data along with its own pressure measurement (P_m) and equation (1) to calculate its altitude (h_c). The calculated altitude, h_c, was compared to the true altitude at the location to generate an altitude error.

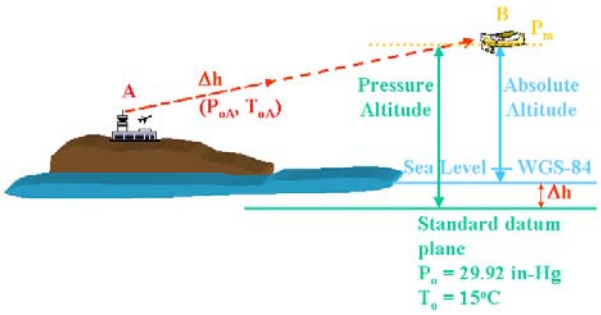

Figure 2. The configuration of our simulation, our simulation assumed that an airplane gets temperature and pressure data from a control tower. This is an example for a non-standard day. In a standard day, the standard datum plane and sea level-WGS84 are the same.

The simulation was exercised on historical meteorological data in [8], that provided an hourly meteorological observation data from selected weather stations in the United States. The source data from *NOAA* provides us the measured temperatures, measured pressures, time, and positions in LLH (Latitude, Longitude, Height) of location A and B. Before we can estimate the altitude error of a barometric altimeter, we must convert the measured temperature and pressure (T_m, P_m) at location A to the temperature and pressure at the level of reference (T_0, P_0) via the following equations (2), (3) based on the perfect gas law [10],

$$\ln\left(\frac{P_m}{P_0}\right) = -\frac{gh}{RT_m} \quad (2)$$

$$T_m = T_0 - \lambda h \quad (3)$$

We selected locations in different regions to run our simulation. Two example regions are discussed in this paper, which are Atlanta, GA and Toledo, OH examples. One example region is shown in Figure 3. We chose one location in each region as the airplane location, in Figure 3, it was Toledo, OH. We collected meteorological observation data at each location for a year. We fed all data into our simulator to estimate the altitude of airplane. We then compared the estimated altitude with the provided true altitude to generate altitude error data. Figure 4 shows an example of altitude error data for an airplane which is at Toledo, OH. The subplots of Figure 4 are in the order of distance between the airplane and the other weather station. For example, the altitude error using the data from the nearest reference station is shown on the top of Figure 4.

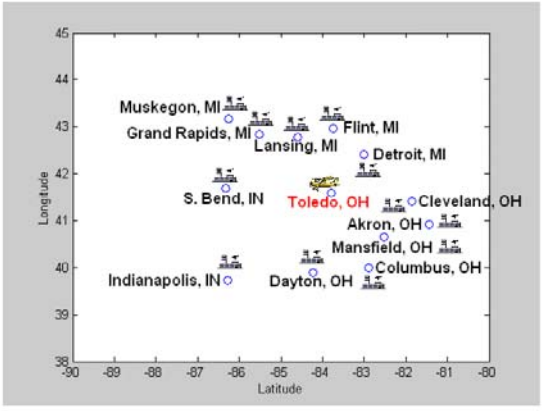

Figure 3. A selected region in U.S.. The red color means that the airplane is at that location, which is Toledo, OH in this example.

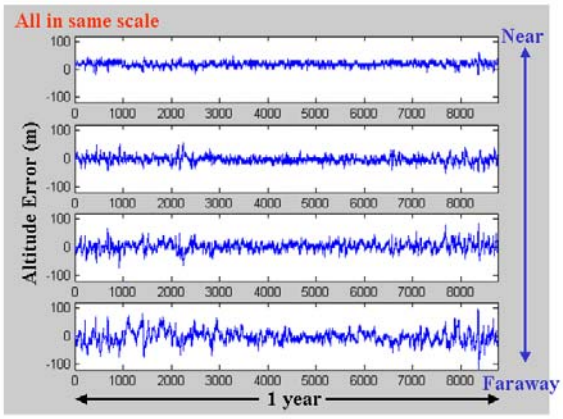

Figure 4. This is an example of altitude error data which is generated from Toledo, OH region.

Figure 4 shows that the altitude error data curve using near weather station's data is smoother than the one using faraway weather station's data, because the near weather station has similar weather pattern as where the airplane is (smaller temperature and pressure variations).

In order to build the barometric altimeter error model, we first calculated the standard deviation (σ) of the altitude error data. We then applied the following linear least square estimation technique to fit a line to the error data.

$$Y = ax + b \qquad (4)$$

where,

Y: Altitude error

a: Distance between place A and place B (Km)

x: slope

b: constant

Re-arrange the equation,

$$Y = [a \quad 1]\begin{bmatrix} x \\ b \end{bmatrix} \qquad (5)$$

$$A = [a \quad 1],$$

$$X = \begin{bmatrix} x \\ b \end{bmatrix}$$

Weighted Least Square Estimation

$$X_{wls} = (A^T W^{-1} A)^{-1} A^T W^{-1} Y \qquad (6)$$

For Atlanta, GA example, we got

$$Y = 0.0639a + 0.0043 \qquad (7)$$

For Toledo, OH example, we got

$$Y = 0.0766a + 0.0049 \qquad (8)$$

The linear estimation results of both examples (7), (8) show us the altitude error is a function of the distance between the airplane and the reference weather station. The result of Atlanta, GA example is shown in Figure 5.

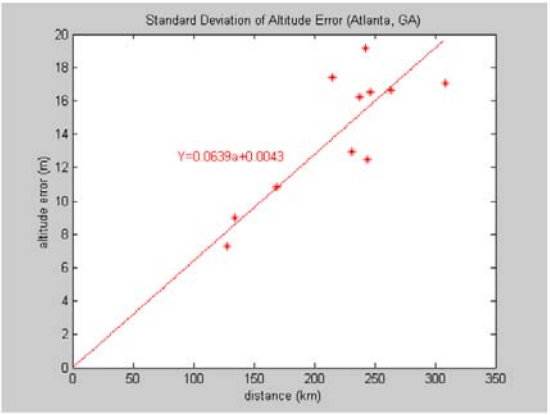

Figure 5. The * is the standard deviation of the altitude error, and the red line shows the result of the linear estimation.

Our goal is to develop the barometric altimeter confidence model. The model of standard deviation of barometric altimeter is not conservative enough for safety of life applications like the ones we are considering in this paper. Instead, we collected the worst-case error of the same data shown in Figure 4, and applied the same linear estimation. The results were the following:

For Atlanta, GA example

$$Y = 0.3070a + 18.5478 \qquad (9)$$

For Toledo, OH example

$$Y = 0.4125a + 20.3868 \qquad (10)$$

The results are shown in Figure 6. In the magnitude of error view, the model of Toledo, OH example (10) is worse than the one of Atlanta, GA (9). As a result, the worst-case model of Toledo, OH is chosen as our confidence model of barometric altimeter. For conservatism, we add 10% as safety factor to equation (10). Thus, our barometric altimeter confidence model is

$$Y = 1.1(0.4125a + 20.3868) \qquad (11)$$

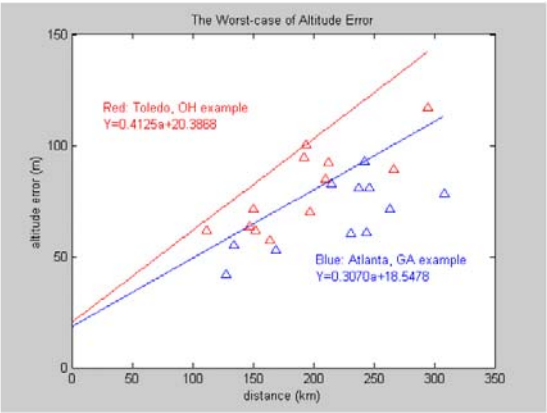

Figure 6. The worst-case model of the barometric altimeter, the blue color part is for Atlanta, GA example, and the red color part is for Toledo, OH example.

Before we apply this confidence model into our further analysis, we must verify it with some data. To this end, we collected 5 years meteorological observation data for the same locations in Toledo, OH example. We then used our MATLAB® simulator to generate the worst-case altitude error data. We used these worst-case errors to test our confidence model (11). As shown in Figure 7, our confidence model successfully bound these worst-case errors. Figure 7 also shows that we could successfully include the worst-case error even without the 10% safety factor.

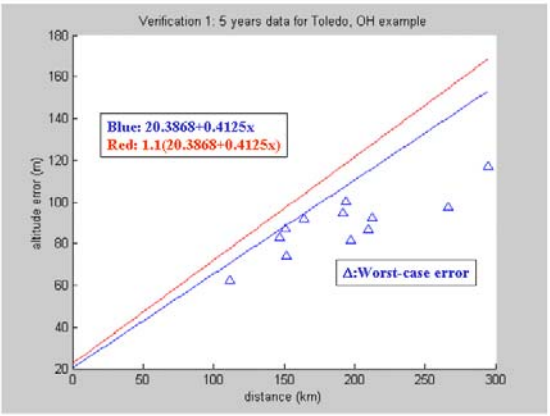

Figure 7, Our confidence model successfully bound these worst-case errors; this Figure also shows that we could successfully bound the worst-case error even without the 10% safety factor.

The second verification of our confidence model, we collected 5 years meteorological observation data for Boston, MA and Worcester, MA. We assumed that the airplane is at Worcester, MA and the reference weather station is at Boston, MA. We then used the same algorithm to generate the altitude error data. The altitude error distribution is shown in Figure 8. The statistics for this distribution are as follows,

Total data points = 43824

Maximum error = 47.1136m

$$\text{Probability(maximum error)} = \frac{1}{43824}$$

Confidence bound=

$$(20.3868+0.4125*66.8812)*1.1=52.7728\text{m}$$

$$\text{Probability(Error} \geq 45\text{m)} = \frac{2}{43824}$$

$$\text{Probability(Error} \geq 40\text{m)} = \frac{6}{43824}$$

$$\text{Probability(Error} \geq 20\text{m)} = \frac{354}{43824}$$

The maximum altitude error is well bounded by our barometric altimeter confidence model (47.1136<52.7728). We will use the barometric altimeter confidence bound of this Boston-Worcester example, which is 52.7728 m, as our barometric altimeter confidence for all analysis and simulation in the rest of this paper.

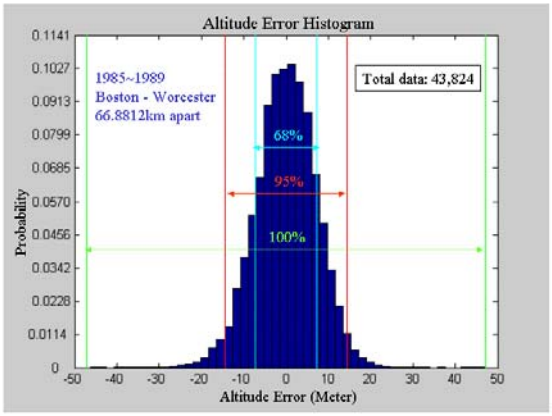

Figure 8. The distribution of altitude error. The maximum error is 47.1136 m and is well bounded by our confidence model which is 52.7728 m.

V. Protection Level Calculation

The protection level calculation is summarized in Figure 9. The detail description of these calculations can be found in WAAS MOPS (RTCA DO-229C) [7]. Previous work in [4] showed that the ionosphere is a significant factor affecting availability, and the conclusion of another study documented in [11] was that 'the only GPS risks that proved significant are interference and ionosphere propagation effects'. As a result, we first investigated the

calculation of user ionosphere range error (UIRE) confidence, which is the yellow highlighted portion in Figure 9. The calculations of other terms will be discussed in a future paper.

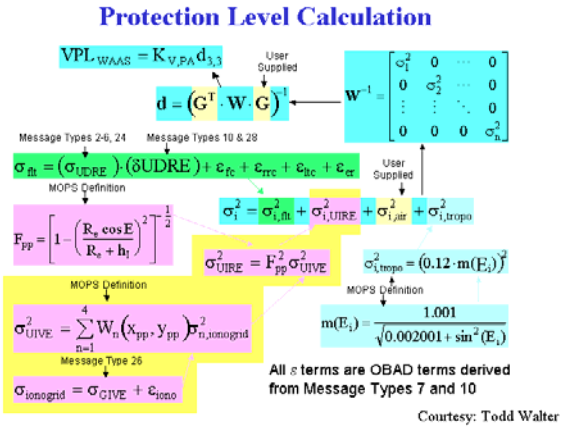

Figure 9. The protection level calculation, only the yellow highlighted portion be discussed in this paper. (See Appendices A and J of RTCA DO-229C) [7]

The WAAS reference station (WRS) dual-frequency measurement of ionosphere delay at L1 [6] is

$$I_{L1} = \frac{f_{L2}^2}{\left(f_{L1}^2 - f_{L2}^2\right)}\left(\rho_{L2} - \rho_{L1}\right) \qquad (12)$$

where,

ρ_{L1} : pseudorange measurement of L1

ρ_{L2} : pseudorange measurement of L2

f_{L1} : GPS L1 frequency (1575.42MHz)

f_{L2} : GPS L2 frequency (1227.6MHz)

I_{L1} : Ionosphere delay at L1

Similarly, the ionosphere delay at L2 is

$$I_{L2} = \frac{f_{L1}^2}{\left(f_{L1}^2 - f_{L2}^2\right)}\left(\rho_{L2} - \rho_{L1}\right) \qquad (13)$$

Compare I_{L1} with I_{L2}, we get

$$\frac{I_{L2}}{I_{L1}} = \frac{f_{L1}^2}{f_{L2}^2} = 1.6469 \qquad (14)$$

Similarly,

For L1 and L5 dual-frequency measurement,

$$\frac{I_{L5}}{I_{L1}} = \frac{f_{L1}^2}{f_{L5}^2} = 1.7933 \qquad (15)$$

that means, the algorithm of UIRE confidence calculation in WAAS is same for single frequency GPS user (L1, L2, or L5), but for L2 or L5 single frequency user, the following modification is required,

For L2 single frequency user,

$$\sigma_{UIVE\_L2} = \sigma_{UIVE\_L1}\left(\frac{f_1}{f_2}\right)^2 \qquad (16)$$

For L5 single frequency user,

$$\sigma_{UIVE\_L5} = \sigma_{UIVE\_L1}\left(\frac{f_1}{f_5}\right)^2 \qquad (17)$$

The changes of UIRE confidence calculation are summarized in Figure 10. The changes of other terms in protection level calculation, such as fast and long term correction degradation confidence (σ_{flt}), airborne receiver confidence ($\sigma_{i,air}$), and troposphere delay confidence ($\sigma_{i,tropo}$) [7], are the subject of on-going research. Therefore, the simulations described in the next section adopted the changes in UIRE, but kept the other terms unchanged.

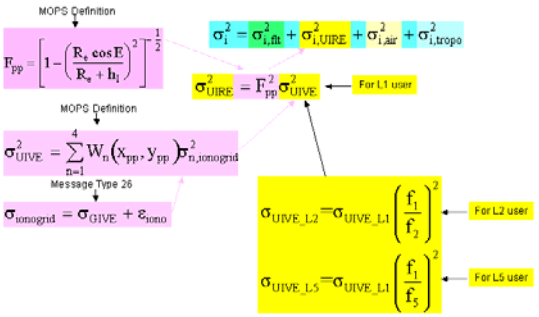

Figure 10. Summary of changes in user ionosphere range error (UIRE) confidence calculation.

VI. Simulation and Results

The criterion of this research is to compare the coverage of availabilities versus the vertical alert limit (VAL) under these cases. The following cases were simulated and evaluated in this paper,

- A single frequency L1, L2, or L5 user with WAAS
- A single frequency L1, L2, or L5 user with WAAS and a barometric altimeter aiding

The simulation tool in this paper is MATLAB® Algorithm Availability Simulation Tool (MAAST) [4], MAAST is a publicly available software tool, which can be customized to simulate the WAAS confidence estimation algorithms and evaluate the effect of service availability with algorithms change. MAAST is available for downloading at *http://waas.stanford.edu*.

Similar to the WAAS protection level calculation, the calculation of ionosphere delay confidence (UIRE) also needs a modification for different GPS frequency users. The *sig2_uive* in *usrprocess.m* of MAAST is multiplied by a scale factor for a L2 single frequency user, which is $(1.6469)^2$ from equation (14). Similarly, a L5 single frequency user used a scale factor of $(1.7933)^2$ from equation (15). The other important parameters used in the simulation are vertical alert limit (VAL) = 50 m, and the horizontal alert limit (HAL) = 40 m.

The simulation results of a L1 single frequency user are shown in Figures 11-13. The simulation results of a L2 single frequency user are shown in Figures 14-16. The simulation results of a L5 single frequency user are shown in Figures 17-19. The 95% shown in Figures 11, 14 and 17, represents the fraction of users within those regions that had a time availability of 95% or greater. The coverage of L1 single frequency user with WAAS is 98.84%, which is better than L2 single frequency user which is 92.28%. It is also better than the coverage of availability for L5 single frequency user which is 87.57%.

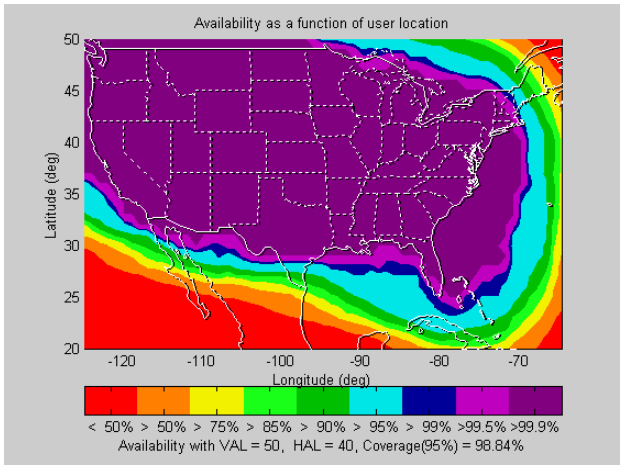

Figure 11. Coverage of L1 single frequency user in CONUS is 98.84% with VAL=50m, HAL=40m.

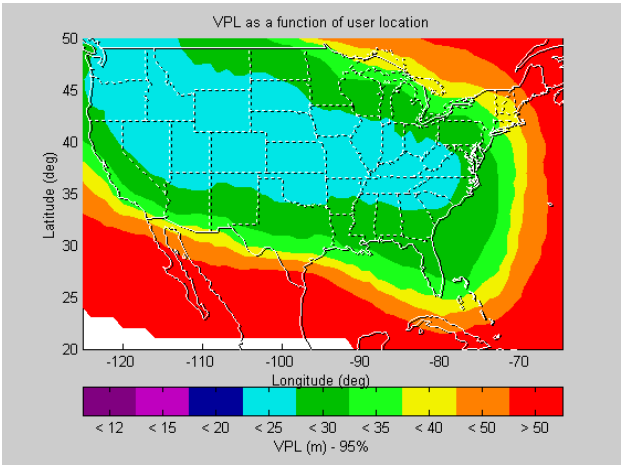

Figure 12. Vertical protection level (VPL) contour of a L1 single frequency user in CONUS.

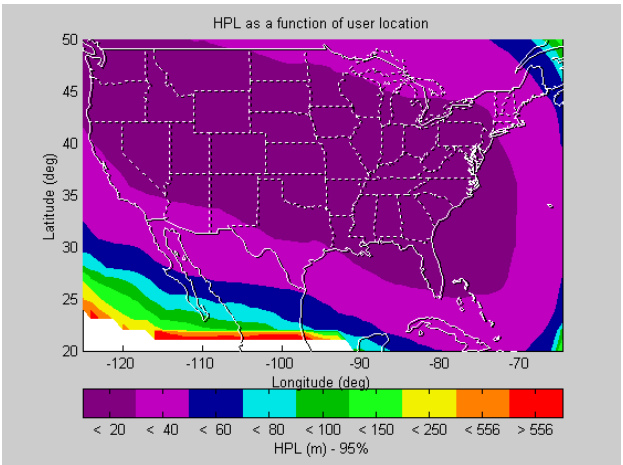

Figure 13. Horizontal protection level (HPL) contour of a L1 single frequency user in CONUS.

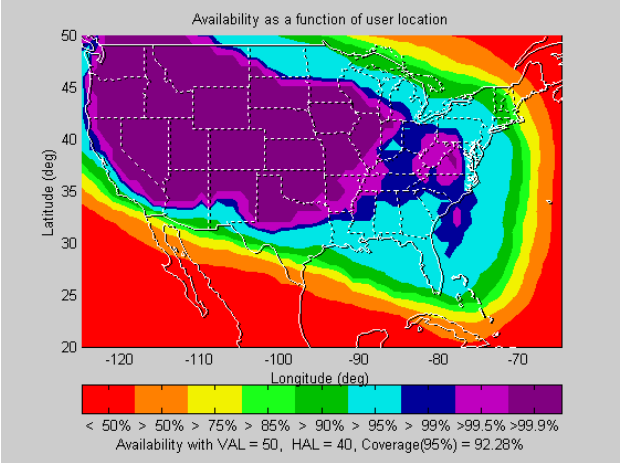

Figure 14. Coverage of L2 single frequency user in CONUS is 92.28% with VAL=50m, HAL=40m.

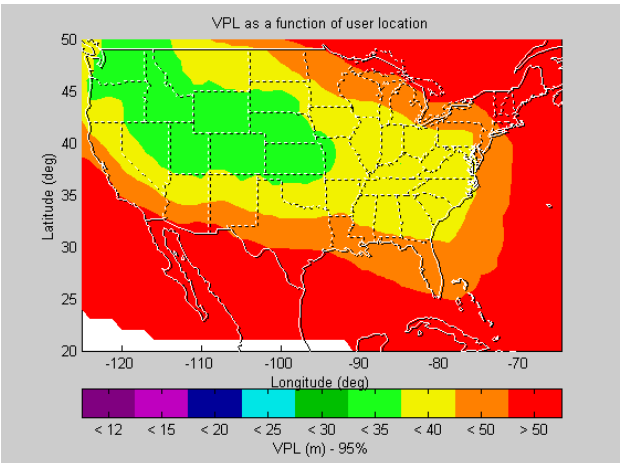

Figure 15. Vertical protection level (VPL) contour of a L2 single frequency user in CONUS.

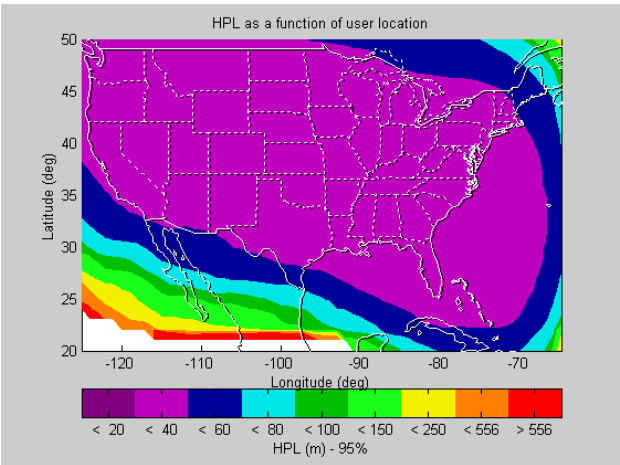

Figure 16. Horizontal protection level (HPL) contour of a L2 single frequency user in CONUS.

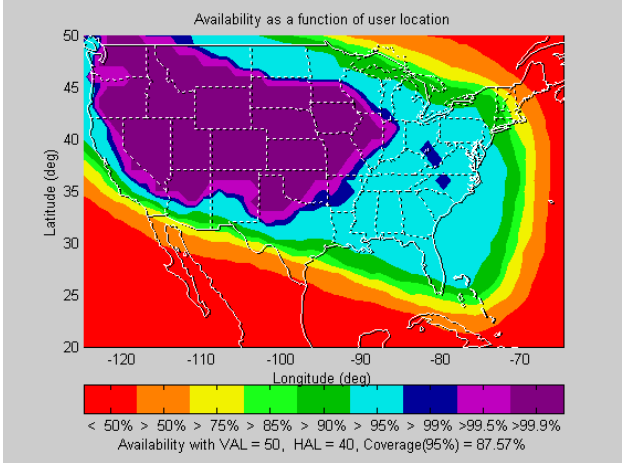

Figure 17. Coverage of L5 single frequency user in CONUS is 87.57% with VAL=50m, HAL=40m.

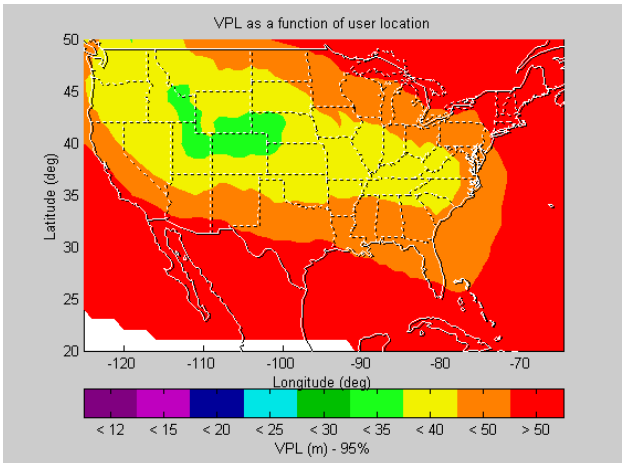

Figure 18. Vertical protection level (VPL) contour of a L5 single frequency user in CONUS.

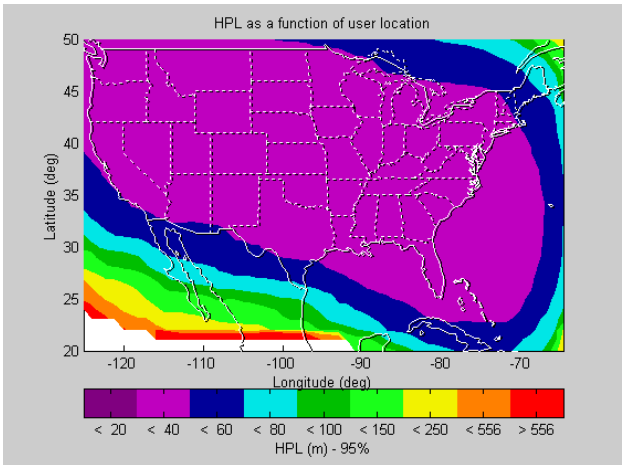

Figure 19. Horizontal protection level (HPL) contour of a L5 single frequency user in CONUS.

For a single frequency GPS user with WAAS and a barometric altimeter cases, we treated the barometric altimeter as a virtual satellite with known clock at the user location when we performed the availability simulation. The GPS observation direction cosine matrix G_{GPS} in the user's local East-North-Up frame was modified to $G_{GPS+Baro}$ to include a barometric altimeter in the following manner:

$$G_{GPS+Baro} = \begin{bmatrix} & G_{GPS} & \\ 0 & 0 & 1 & 0 \end{bmatrix} \qquad (18)$$

The weighting matrix W in the protection level calculation (shown in Figure 9) was modified to include the barometric altimeter confidence (σ_{baro}) [7],

$$W = \begin{bmatrix} \sigma_1^{-1} & 0 & \dots & 0 \\ 0 & \sigma_2^{-1} & \dots & 0 \\ \dots & \dots & \dots & \dots \\ 0 & 0 & \dots & \sigma_{baro}^{-1} \end{bmatrix} \qquad (19)$$

In this paper, the confidence of a barometric altimeter is calculated using data from the Boston-Worcester example discussed earlier,

$$\sigma_{baro} = \frac{52.7728}{5.33} = 9.9011(m) \qquad (20)$$

Where,

5.33 is the K_{HMI} value defined in Appendix J of the MOPS [7]

In MAAST, we modified the *usr_vhpl.m* based on the equations (18), (19) and (20). The simulation results of L1 single frequency WAAS user with barometric altimeter aiding are shown in Figure 20-22. The simulation results of L2 single frequency WAAS user with barometric altimeter aiding are shown in Figure 23-25. The simulation results of L5 single frequency WAAS user with barometric altimeter aiding are shown in Figure 26-28.

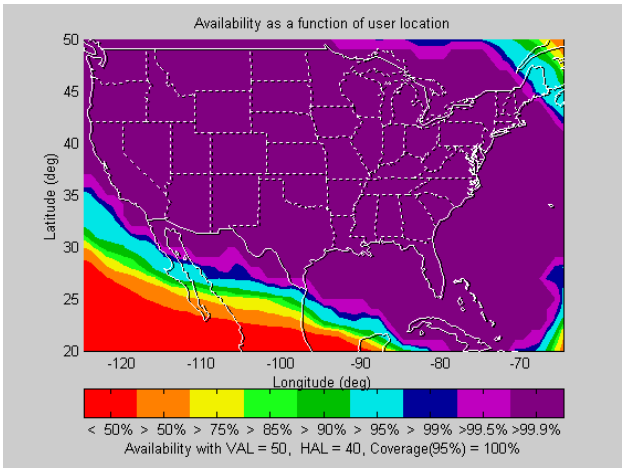

Figure 20. Coverage of L1 single frequency user with barometric altimeter aiding in CONUS is 100% with VAL=50m, HAL=40m.

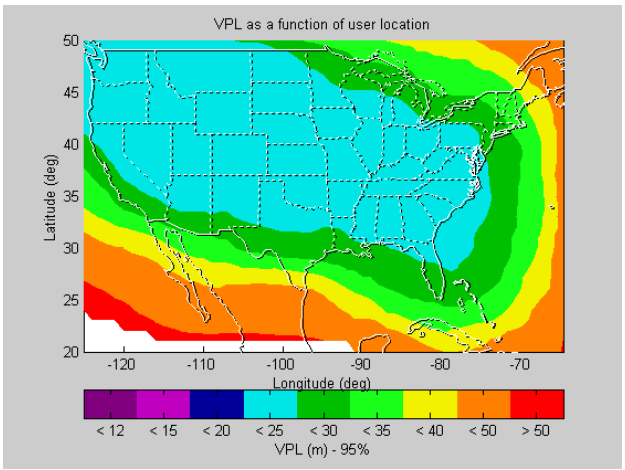

Figure 21. Vertical protection level (VPL) contour of a L1 single frequency user with barometric altimeter aiding in CONUS.

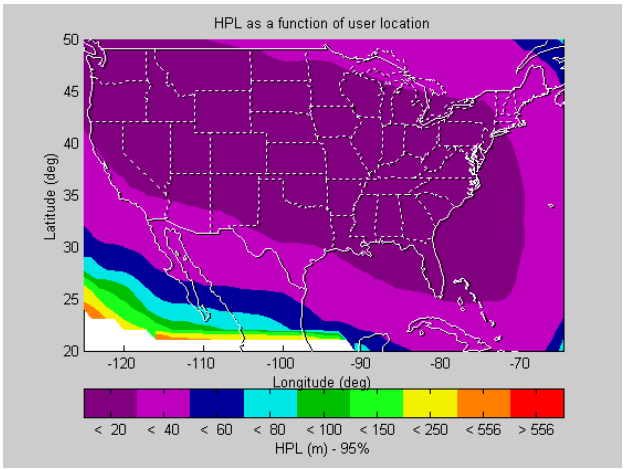

Figure 22. Horizontal protection level (HPL) contour of a L1 single frequency user with barometric altimeter aiding in CONUS.

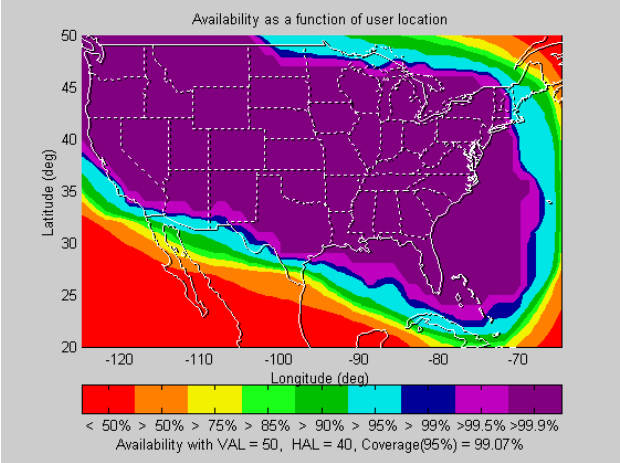

Figure 23. Coverage of L2 single frequency user with barometric altimeter aiding in CONUS is 99.07% with VAL=50m, HAL=40m.

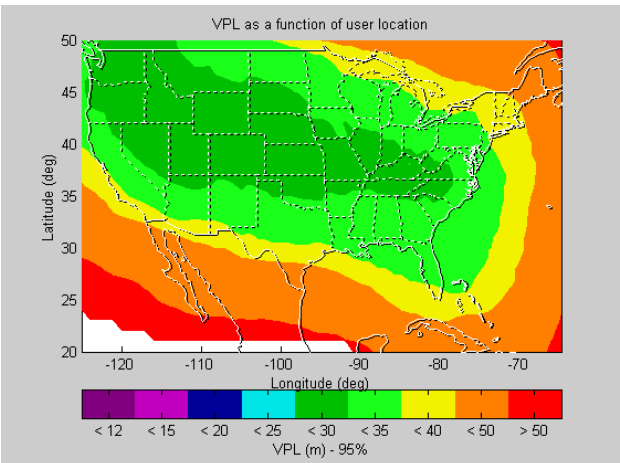

Figure 24. Vertical protection level (VPL) contour of a L2 single frequency user with barometric altimeter aiding in CONUS.

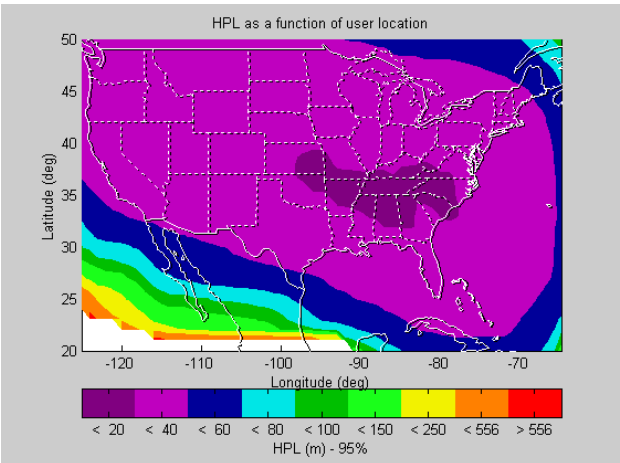

Figure 25. Horizontal protection level (HPL) contour of a L2 single frequency user with barometric altimeter aiding in CONUS.

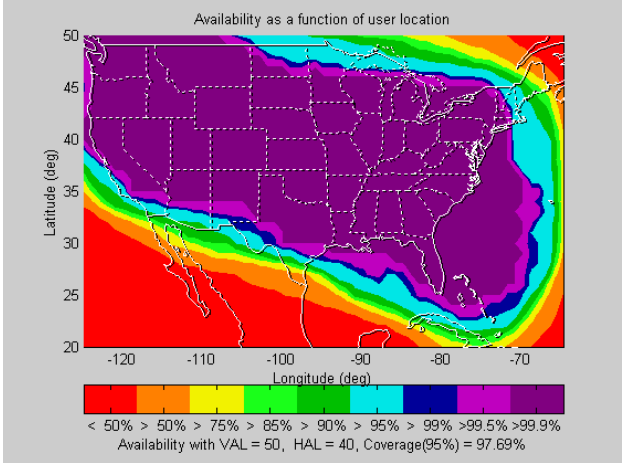

Figure 26 Coverage of L5 single frequency user with barometric altimeter aiding in CONUS is 97.69% with VAL=50m, HAL=40m.

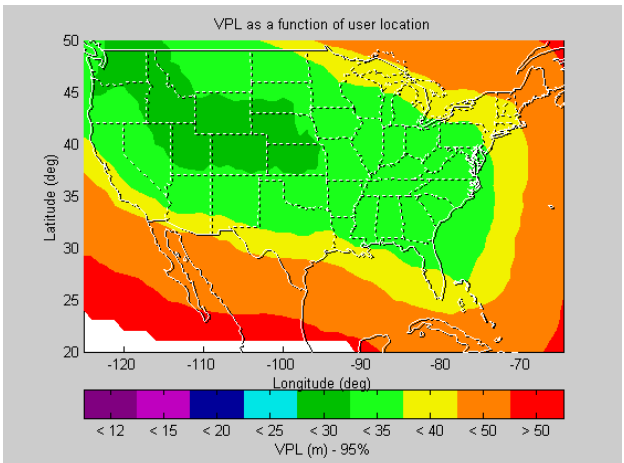

Figure 27. Vertical protection level (VPL) contour of a L5 single frequency user with barometric altimeter aiding in CONUS.

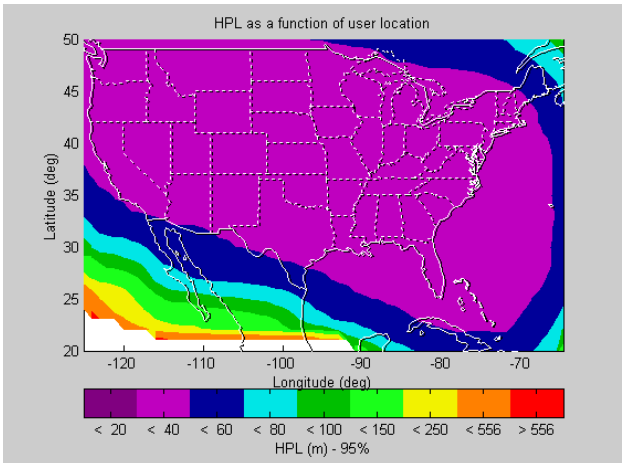

Figure 28. Horizontal protection level (HPL) contour of a L5 single frequency user with barometric altimeter aiding in CONUS.

The Coverage of L1 single frequency user with WAAS and a barometric altimeter aiding is 100%, which is better than L2 single frequency user with WAAS and a barometric altimeter aiding which is 99.07%, and also better than L5 single frequency user with WAAS and a barometric altimeter aiding which is 97.69%. A summary of these results is shown in Table 1.

Table 1. Summary of the coverage of a single frequency user with WAAS and a barometric altimeter.

	w/o Barometric altimeter aiding	w/ barometric altimeter aiding	improvement
L1 single frequency user	98.84%	100%	1.16%
L2 single frequency user	92.28%	99.07%	6.79%
L5 single frequency user	87.57%	97.69%	10.12%

VII. Conclusion and Future Work

We have used MAAST to analyze the coverage of the single frequency GPS user with WAAS both with and without barometric altimeter aiding. Because the barometric altimeter acts as a virtual satellite about the user location, barometric altimeter information is extremely beneficial, primarily in the vertical. It is particularly useful when other satellites have bad geometry.

The effects of WAAS L1 correction for a L2 or L5 single frequency user UIRE confidence calculation were also discussed in this paper. The results of these analysis are shown in the first column of Table 1. In summary, the lower GPS frequency has larger ionosphere delay uncertainty, therefore, the L1-only user has highest single frequency availability. Thus, to minimize the ionosphere delay effect, a higher GPS frequency (higher than L1) is preferable when selecting new GPS frequency in GPS modernization. MAAST simulation results also show that WAAS ionosphere delay correction would allow an airplane to land in the worst-case scenarios.

The next step will be to investigate the effects of other terms in protection level calculation for different single frequency user. For example, fast and long term correction degradation confidence (σ_{flt}), airborne receiver confidence ($\sigma_{i,air}$), and troposphere delay confidence ($\sigma_{i,tropo}$) need to be evaluated. The cases of a dual-frequency GPS user (L1-L2, L1-L5, and L2-L5) will also be investigated in the future.

The assumptions about the confidence model of a barometric altimeter in this paper are that air is perfect gas, and that the linear relationship for temperature lapse rate holds. These assumptions might introduce some error. As a result, in the future a new confidence model of a barometric altimeter will be developed based on the flight test data.

Acknowledgement

Authors would like to thank the Federal Aviation Administration (FAA) for supporting this research.

References

1. Dobyne, J., "The Accuracy of Barometric Altimeters with Respect to Geometric Altitude," *Proceedings of ION Satellite Division's International Technical Meeting 1988*, Springs, CO, September 19-23, 1988.
2. Enge, P., Walter, T., Pullen, S., Kee, C., Chao, Y.-C., Tsai, Y.-J., "Wide Area Augmentation of The Global Positioning System," *Proceedings of the IEEE, Volume: 84 Issue: 8*, August, 1996.
3. ICD-GPS-200C, *NAVSTAR GPS Space Segment / Navigation User Interface*, Arinc Research Corporation, El Segundo, CA, October 10, 1993, and subsequent IRNs 1 through 4, April 12, 2000.
4. Jan, S.-S., Chan, W., Walter, T., Enge, P., "MATLAB Simulation Toolset for SBAS Availability Analysis," *Proceedings of ION GPS 2001*, Salt Lake City, UT, September 11-14, 2001.
5. Lee, Y. C., "Receiver Autonomous Integrity Monitoring Availability for GPS Augmented with Barometric Altimeter Aiding and Clock Coasting," *Global Positioning System: Theory and Application II*, AIAA, 1996.
6. Misra, P., Enge, P., *Global Positioning System Signal, Measurements, and Performance*, Ganga-Jamuna Press, Lincoln, MA, 2001.
7. RTCA SC-159, *Minimum Operational Performance Standard for Global Positioning System/Wide Area Augmentation System Airborne Equipment*, RTCA/DO-229B, October 6, 1999.
8. *Solar and Meteorological Surface Observation Network 1961-1990*, V. 1.0, NOAA, U. S. Department of Commerce, September, 1993.
9. Van Dierendonck, A. J., "Signal Specification for the Future GPS Civil Signal at L5," *Proceedings of ION Annual Meeting 2000*, San Diego, CA, June 26-28, 2000.
10. Von Mises, R., *Theory of Flight*, Dover, 1959.
11. *GPS Risk Assessment Study*, Applied Physics Laboratory, Johns Hopkins University.